MM Science Journal | www.mmscience.eu
ISSN 1803-1269 (Print) | ISSN 1805-0476 (On-line)
Special Issue | HSM 2025
18th International Conference on High Speed Machining
October 15-16, 2025, Metz, France
DOI: 10.17973/MMSJ.2025_11_2025143

HSM2025-44842

INFLUENCE ON THE QUALITY OF MICROMILLING CHANNELS IN TITANIUM ALLOY PRODUCED OVER ABRASIVE WATERJET MACHINED SURFACES

F. Carretta[1,2]*, A. C. Araujo[2], L. Crouzeix[2]
[1]Politecnico di Milano, Milan, Italy
[2]Institute Clement Ader (ICA), Universite de Toulouse, CNRS/INSA/ISAE/Mines Albi/UPS, Toulouse, France
*Corresponding author(s); e-mail: filippo.carretta@mail.polimi.it

Abstract
Titanium alloys are widely employed in several industrial applications, including medical sector thanks to their biocompatibility, and are useful when high strength-to-weight ratio, high temperature and corrosion resistance are desirable. Since titanium alloys have considerably low thermal conductivity and high hardness, thus being difficult to machine, abrasive water-jet machining (AWJM) represents an interesting technology to preserve the material's properties, as it also reduces the damage caused by material overheating. In order to obtain micro details for precision engineering, micromilling with micro-ball end mills can be used as a secondary process to refine the surface previously obtained. However, the existing literature lacks in-depth studies on the micromilling process applied to previously AWJ-machined pockets. The aim of this study is to analyze the surface quality of the channels after these two machining processes comparing the results obtained with workpieces without AWJ-machined pockets. To assess the quality of the specimens, surface roughness, burrs formation and dimensional accuracy are investigated. Furthermore, this research aims to offer practical recommendations to optimize the sequential use of hybrid advanced machining strategies for titanium alloys to highlight their potential in high-precision applications.

Keywords:
Titanium alloy, Abrasive Waterjet, Micromilling, Surface finish, Burr formation

1 INTRODUCTION

Titanium alloys have become increasingly preferred in various industrial sectors including aerospace, oil and gas, automotive, and due to biocompatibility, also biomedical, and in general in applications that require high fatigue resistance as well as low density and corrosion resistance.

In this study, the machining of Ti6Al4V titanium alloy was analyzed, which is one of the most employed α/β titanium alloy in industry. According to ASTM (American Society for Testing and Materials), the chemical composition of Ti6Al4V consists of aluminum (Al) 5.5–6.75 wt%, vanadium (V) 3.5–4.5 wt%, iron (Fe) 0–0.4 wt%, carbon (C) 0–0.1 wt%, hydrogen (H) 0–0.0125 wt%, nitrogen (N) 0–0.05 wt%, oxygen (O) 0–0.2 wt%, and other elements up to 0.4 wt%, with a balance in titanium (Ti) content typically 88-91 wt%.

Due to the thermomechanical properties of Ti6Al4V, including mainly low thermal conductivity, hardness retention at high temperature, high chemical reactivity with the majority of tool materials, and with a strong tendency toward galling during machining, this alloy has been recognized in literature as a difficult to cut material for traditional machining processes, such as milling, drilling and turning, leading to lower tool life, poorer surface finish, wider HAZ (heat affected zone) due to limited heat dissipation in the cutting zone [Niknam et al. 2014], [Veiga et al. 2013].

Abrasive waterjet (AWJ) technology using a combination of pressurized water and abrasive particles to remove material, represents a favorable unconventional machining process for Ti6Al4V being a cold process, thus avoiding HAZ, limiting the deformation of workpieces during machining thanks to decreased specific cutting forces, and preserving the mechanical properties of the titanium alloy [Bui et al. 2017], [Bui et al. 2019].

Moreover, complex shapes such as pocket milling and channels milling are feasible with AWJ, and especially when parts are wide and thin, as in the case of plates, traditional processes for material removal of titanium alloys may not guarantee strict geometrical specifications due to the previously mentioned challenges in machining [Bui et al. 2017], [Bui et al. 2019].

Moreover, the increasing demand of miniaturized components, the detail-oriented design that has been recently a growing trend in industrial application of metal cutting, has brought to extensive research on the micromilling process [Dornfeld et al. 2006]. Micromilling on Ti6Al4V, allows to achieve miniaturized features, low surface roughness, reduced waviness, rapid fabrication of complex shapes with a low set-up cost, with a high aspect ratio in components [Carou et al. 2017], [Kim et al. 2017], [Thepsonthi et al. 2014] and such considerations are the driving factors of the present study, which aims to evaluate the compatibility of the AWJ process and the micromilling process in a sequential perspective. Furthermore, there are numerous published studies on the optimization of micromilling on Ti6Al4V, ranging from tool wear analysis, forces prediction, vibrations reduction in machining, online real time process monitoring, and many others [Balázs et al. 2021], [Carou et al. 2017], [Dornfeld et al. 2006], however there is a gap in the existing literature on micromilling performed on previously AWJ-machined components.

Besides, the combination of AWJ technology and micromilling, could be an interesting fabrication method for improving the production of microfluidic biomedical components in the form of concave microwells, and microfluidic channels [Jun et al. 2019].

This experimental article developed the following steps:

- AWJ machining of pockets on Ti6Al4V alloy: comparable in size and their depths are predictable using a simple analytical model.
- Optical microscopic analysis of the machined surfaces in terms of geometrical accuracy and surface roughness to determine the best and the worst conditions for the consecutive micromilling process.
- Response Surface Methodology (RSM) on the AWJ experiments to study the statistical influence and relevance of the AWJ process parameters on the metrology of the pockets.
- Dry micromilling of straight lines, and then dry micromilling with a complex path (spiral) with a ball end mill on the AWJ machined pockets.
- Optical microscopic analysis of the surface integrity in terms of geometrical accuracy and burrs presence.

2 EMPIRIC MODELING OF AWJ EXPERIMENTS

This section presents the empirical analytical modeling aiming at creating AWJ machined pockets with a depth of approximately 1 mm, comparable to each other, using different AWJ process parameters.

There are some fixed parameters to be chosen in AWJ: the abrasive material, the mesh (#) of the abrasive particles, as well as the abrasive mass flow rate ($\dot{m}_a$). The variable parameters of the AWJ process include: pressure (*P*), stand-off distance (*SOD*), pitch (*pi*), and feed rate (v_f).

In order to identify the parameters for a model to predict a suitable v_f for obtaining the desired depth (*h*) of the AWJ milled pockets, a nonlinear least squares approach based on the Generalized Reduced Gradient (GRG) method was employed based on the following equations [Sultan 2015]:

$$h = a \cdot (P)^b \cdot (SOD)^c \cdot (pi)^d \cdot (v_f)^e \quad (1)$$

$$v_f = \sqrt[e]{\frac{h}{a \cdot (P)^b \cdot (SOD)^c \cdot (pi)^d}} \quad (2)$$

By setting a target depth equal to 1 mm, the model shown in Eq. (2) can be used to determine an optimal feed rate (v_f) for any given combination of input parameters. The *a*, *b*, *c*, *d*, and *e* coefficients are determined through nonlinear regression. A limitation of the presented model lies in its sensitivity to the first guess for the variable to be optimized, which affects the reliability and convergence of the results. Therefore, the initial v_f equal to 2100 mm/min has been chosen according to literature for similar parameters and settings [Bui et al. 2017] and it has been used as the first guess for the optimization of the v_f variable.

Similar nonlinear models have been proposed in literature for AWJ machining on Ti6Al4V alloy, for instance [Sultan 2015] developed a study in which it is presented a predictive model for the AWJ milled pocket width, where the input parameters include the abrasive's granulometry and not the pitch. Also, [Bui et al. 2017] proposed a similar model for predicting depth in AWJ milling by taking into consideration the effect of jet inclination. In addition, [Kumar et al. 2025] developed an accurate model to predict the AWJ milled channels geometry by manipulating feed rate and jet impingement angle.

3 EXPERIMENTAL POCKETS IN AWJ

The AWJ machine FLOW MACH4-C with a PASER4 cutting head has been used in the experiments. It is composed of a standard 0.33 mm nozzle, and a focusing tube with a diameter of 1.016 mm and a length of 101.6 mm. The machine allows to tilt the cutting head, but in these experiments only three axis movements have been implemented. Moreover, the HYPLEX-PRIME pump can pressurize water up to 400 MPa.

In the CNC there are two installed software: FLOWPATH, which allows path planning (with the scheme shown in Fig. 1), and FLOWCUT, which allows to control and setup the process parameters. Garnet #120 abrasives have been used for these experiments, whose abrasive mass flow rate of 419 g/min has been achieved by means of a 0.215 mm metering disk.

The specimens of 20x100x5 mm were cut using the same AWJ machine from a titanium block. Before performing the AWJ milling operations the specimens were grinded with a JET PROMAC 315BE1 grinding machine. To clamp the specimens to a flat wooden plate, screws and washers were used, to ensure the workpiece is securely fixed.

In Fig. 1 all the relevant information on the experimental setup employed are schematized and presented.

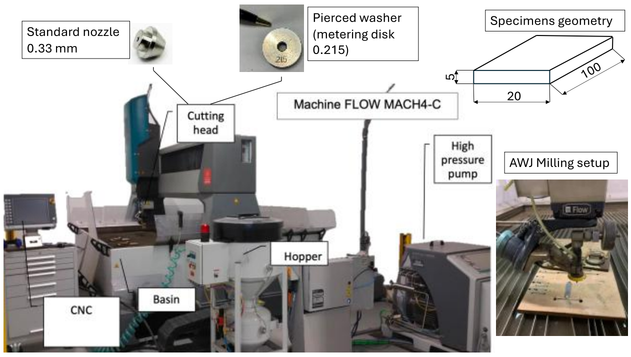

Fig. 1: Experimental setup

Therefore, a Taguchi 3x3 orthogonal array, with an extra run has been designed, and the three factors, that are pressure (*P*), stand-off distance (*SOD*), and pitch (*pi*) with their three levels, as well as fixed and variable selected parameters are shown in Fig. 2.

4 RESULTS OF THE GEOMETRY OF POCKETS

The objective of this section is to present the geometrical measurements of the pockets created through the experiments described in the previous section. Moreover, the objective of the following measurements was to identify the process conditions resulting in the lowest and highest surface roughness, representing the best and worst cases, respectively. These conditions were selected for replication, as they will be used in subsequent micromilling experiments to assess the tool's performance on surfaces with different roughness levels.

Factors and levels			
Run	Pressure (P) [bar]	Stand-off distance (SOD) [mm]	Pitch (pi) [mm]
#1	3500	65	1
#2	3500	100	0.5
#3	3500	40	0.75
#4	1000	40	0.5
#5	1000	65	0.75
#6	2250	100	0.75
#7	1000	100	1
#8	2250	40	1
#9	2250	65	0.5
#10	2250	100	0.5

Fixed parameters	
Measured abrasive mass flow rate ($\dot{m}_a$) [g/min]	419
Abrasive type and size	Garnet #120

Variable parameter
Feed rate (v_f) [mm/min]

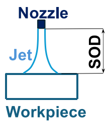

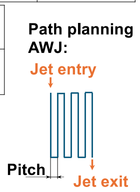

Fig. 2: D.O.E. and process parameters

4.1 Optical measurements

Infinite-Focus Measurement (IFM) equipment Alicona IF SL has been used in this study to perform 3D optical measurements using 10x lens. Using this equipment it was measured: geometrical features and topographical characteristics of the AWJ milled channels, the average roughness of profiles (R_a), the mean peak to valley height of roughness profile (R_z), and, for texture, the average height of the flat bottom areas (S_a).

The embedded software allows to perform pocket measurements following the ISO 5234, as shown in Fig. 3, that are the horizontal red lines in the graphical surface reconstruction. Starting from these red lines the depth of the pocket can be measured which has been defined as *h*, that is the vertical distance between the two red lines (Fig. 3).

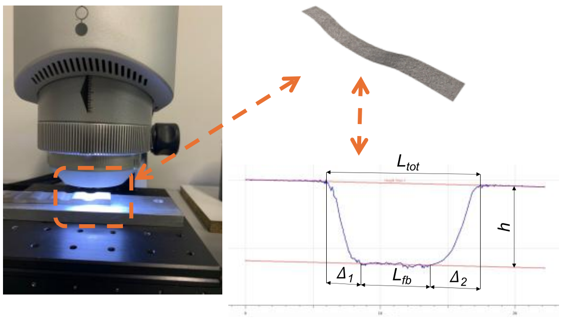

Fig. 3: Infinite-Focus Measurements (Optical in 3D)

Moreover, some geometrical parameters have been defined, namely L_{tot} that is the total length of the pocket, L_{fb} called length of flat bottom, which is an important parameter for the subsequent micromilling experiments since it represents the region where the bottom of the pocket is nearly flat, making it more suitable for subsequent micromilling steps, as the tool is less likely to experience instability or failure compared to areas near the pocket edges, and it is measured as the region which intersects the red horizontal line in the bottom (Fig. 3).

In order to identify the zones outside of the flat bottom, it has been defined a length ratio (*LR*) between the inclination length, Δ_1 and Δ_2, and the pocket depth.

$$LR = \frac{\bar{\Delta}}{h} \quad (3)$$

$$\bar{\Delta} = \Delta_1 + \Delta_2 \quad (4)$$

The *LR* is a quantity which determines if the slope created by the jet has a gentler inclination, that is for higher values of the *LR*, conversely, for lower *LR* values, the pocket is more pronounced, with steeper walls.

4.2 Geometrical and surface roughness result

Four replications were performed according to the pockets with the lowest and highest surface roughness (R_a, R_z, and S_a). The key results are summarized in Fig. 4. For the sake of clarity, only the R_a results are shown, as R_z, and S_a followed the same trends and led to the same best and worst conditions.

The lowest roughness was obtained with low pressure, low *SOD*, and low pitch.

The highest roughness occurred with high pressure, high *SOD*, and low pitch.

AWJ main results			
Run	h [mm]	LR	Ra [µm]
#1	1.044	5.85	8.16
#2	1.034	7.68	8.56
#3	1.191	5.27	4.96
#4	0.939	8.70	2.27
#5	0.734	12.35	3.60
#6	0.999	9.37	5.43
#7	0.758	15.72	4.10
#8	1.102	7.13	3.93
#9	1.127	7.34	5.99
#10	0.912	9.74	6.02

AWJ replications main results			
Run	h [mm]	LR	Ra [µm]
#11	1.09	8.73	7.76
#12	1.00	8.27	2.62
#13	1.07	8.69	8.72
#14	0.98	8.76	2.76

Best
Worst

Fig. 4: Results of the AWJ pockets

4.3 Assessment of the depth prediction model

The objective of this model is to predict the depth of the AWJ-milled pockets based on the process parameters, as defined in Eq. (2) and discussed in Section 2. The model was evaluated using the Root Mean Square Error (RMSE), calculated over 14 experimental data points, resulting in an RMSE of 0.1203 mm.

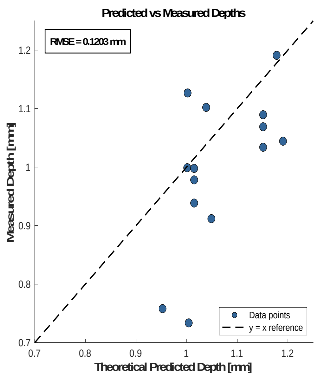

Fig. 5: Depth model evaluation

This level of error is considered acceptable for estimating pocket depth in the context of comparable AWJ milling operations, especially considering the nonlinear nature of the process and the complexity involved. The GRG optimization method was used to fit the model, and further improvements could be made by increasing the number of data points.

Fig. 5 shows a comparison between the predicted depths and the measured (*h*) values. Most data points align closely with the identity line, indicating reasonable model accuracy. However, some deviations can be noticed, suggesting that a larger dataset could enhance the model's predictive capability.

4.4 Response Surface Methodology

The aim of the following Response Surface Methodology (RSM) analysis is to assess the influence of process parameters on the measured responses and to evaluate the quality of the model fits.

To perform the RSM for the experiments, the statistical analysis software JMP Pro 17 has been used with the standard least squares (effect screening) model type, and the main outcomes are summed up in Fig. 6, while in Fig.

7, Fig. 8, and Fig. 9 are reported the main interaction plots calculated from the model, which show visually the influence of the three studied factors.

AWJ – RSM main results					
Response	**ANOVA table p-value**	**Adj. R^2**	**Mean of response**	**RMSE**	**Significant factors (p-value<0.05)**
Depth	0.0028	0.9499	0.9981	0.0292	*P*; *SOD*; *P*P*
Length Ratio	0.0011	0.9692	8.8240	0.4605	*P*; *SOD*; *P*P*
S_a	0.0005	0.9793	6.5060	0.4353	*P*; *SOD*

Fig. 6: RSM main results

Fig. 6 to 9 present three representative responses: *h*, *LR*, and S_a. Conversely, the roughness parameters R_a and R_z have been omitted for the sake of simplicity and also as their trend has proven to be consistent and very similar to the S_a. The three presented models are statistically significant, with ANOVA p-values below 0.01, and they demonstrate strong fits, as their adjusted R^2 values are ranging from 0.95 to 0.98. Moreover, RMSE results confirm that the model has a reasonable prediction capability. Among the investigated factors, pressure, stand-off distance, are the most significant across all responses, and the quadratic effects of pressure are influential for the depth and length ratio responses. Thus, the process is sensitive to pressure, and stand-off distance variations, while the pitch has shown no statistical relevance. The displayed curves suggest that in these experiments higher *P* led to higher *h*, lower *LR*, and higher roughness. Conversely, higher *SOD* resulted in lower *h*, higher *LR* and higher roughness.

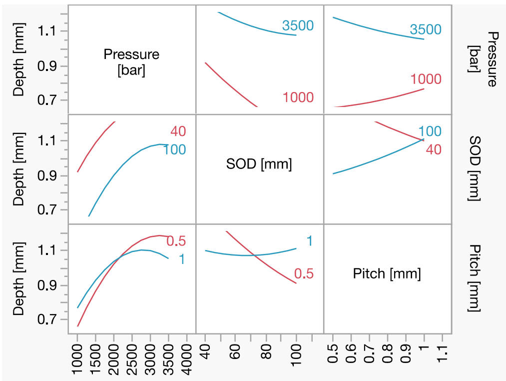

Fig. 7: RSM depth variable interaction plots

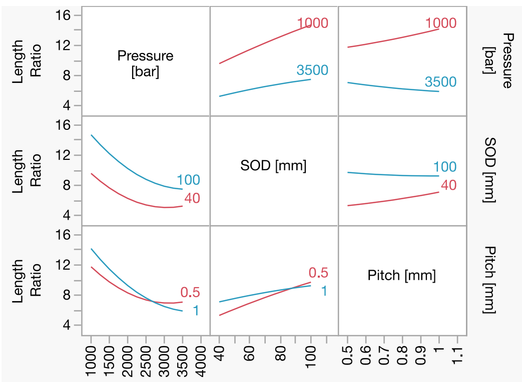

Fig. 8: RSM length ratio variable interaction plots

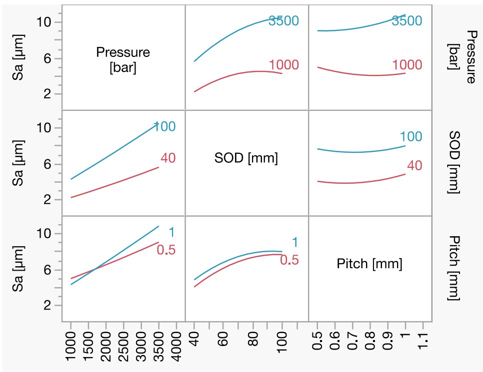

Fig. 9: RSM S_a variable interaction plots

5 MICROMILLING EXPERIMENTAL STRATEGY

5.1 Experimental plan

To define the best parameter for micromilling experiments in the previously AWJ milled pockets, 4 mm straight lines have been machined on a Ti6Al4V workpiece, taken as a reference for evaluating several characteristics of micromilling: geometrical accuracy, chip formation, and presence of burrs. In particular, the focus has been on two process parameters: feed per tooth (f_z) and cutting speed (v_c). Moreover, the micromilling tool employed is a micro-ball-end mill of 0.6 mm diameter.

To assess the best parameters nine different trials have been made on a flat Ti6Al4V reference surface (Tab. 1).

Tab. 1: Micromilling experiments on flat surface

Trial	v_c [m/min]	f_z [µm/tooth]
#1	10	5
#2	20	5
#3	10	10
#4	20	10
#5	10	5
#6	10	10
#7	20	5
#8	15	10
#9	15	5

After the evaluation of the best combination of feed per tooth and cutting speed for the micromilling process, four straight lines in the best and worst replicated pockets (highlighted in section 4.2), one straight line in each pocket, in the direction parallel to the original jet pass has been machined with the same tool, to test the two process parameters also on the previously AWJ pockets.

Thereafter, a specific machining tool path has been designed to investigate the potential of micromilling on the AWJ milled channels with a complex trajectory, that is a spiral. The spiral's geometry has been defined by limiting the axial depth of cut (a_p) to 0.12 mm, to avoid tool breakage during machining. In Fig. 10 are presented the three steps followed in the micromilling experiments.

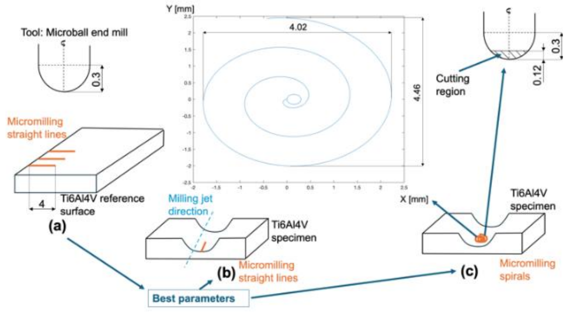

Fig. 10: Micromilling experimental plan: straight path (a) without (b) and with AWJ (c) Spirals

5.2 Experimental setup

To conduct the micromilling experiments, two 5 axes milling machines were used, namely: the DMU 85 Deckel Maho, that has a maximum spindle speed of 30000 rpm, and it has been used to perform the first trials in the reference surface to establish the best parameters, and the Huron U-MILL 5, with a maximum spindle speed of 18000 rpm, has been used to perform the micromilling experiments on the previously AWJ machined channels.

The two machines used in this research have high inertia and stiffness, thus are suitable also for machining large and heavy workpieces. Hence, some limitations had to be addressed, namely: low allowable spindle speed, as machines designed for micromilling operations can reach a maximum speed of 200000 rpm and above [Balázs et al. 2021], then when following a complex toolpath like a spiral, the small curved movements may result in unacceptable errors in machines with big inertia, thus the N40 SOFT UNICODE command has been included to smooth the tool trajectory, and the built-in measurements systems for tool measurements (a laser in the case of DMU 85 Deckel Maho) may not be sensitive enough to tools smaller than 1 mm leading to the need of precise optical measurements, and in the case of this study, of minor , using the 5 axes of the machines, of angles between 0 and 2°.

The optical measurements systems used for the micromilling experiments outcomes were three: Alicona InfiniteFocus SL (shown also in paragraph 4.1), Keyence VX7000 Digital Microscope for assessments of burrs presence, and Micro Vu Vertex 251HM was used for chips analysis.

The micromilling experiments of this study are always in dry cutting, without the use of lubricants. In Fig. 11 are presented the set-ups for the micromilling experiments.

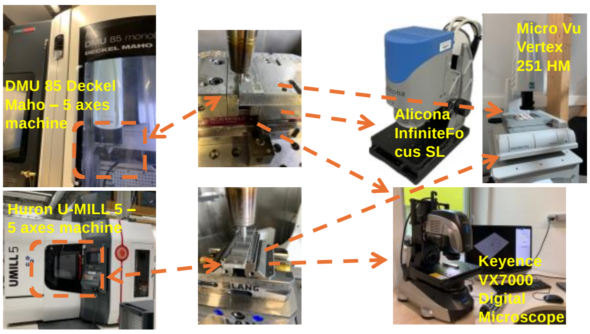

Fig. 11: Setup for micromilling experiments

6 MICROMILLING RESULTS

In Fig. 12 the outcomes of the micromilled straight lines on the flat reference surface in terms of burrs are shown, and the parameter combination which resulted in the lowest burr presence is (according to Tab. 1) the number #1 and #5 Therefore, this combination has been chosen as the best parameter perform our dry cutting experiments also on the previously AWJ milled pockets.

Moreover, in Fig. 13 are presented the chips collected after the micromilling experiments to compare the effect of different parameters, and visually the cutting speed does not show influence in chip formation, and the lower feed per tooth (5 µm/tooth) produced slightly longer and more connected chips. In terms of geometrical accuracy, the micromilled straight lines on the flat reference surface have been measured in three different locations: one at the start of the path, one in the middle, and one before the end of cut.

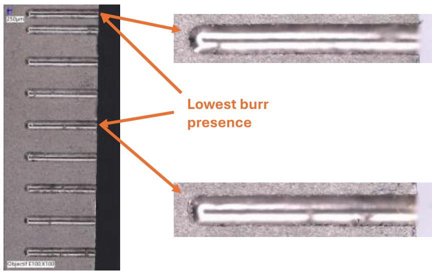

Fig. 12: Burrs presence in micromilling channels

As can be seen in Fig. 14, the experiments showed consistent results in terms of width and in terms of depths over the increasing machining length, using the same tool for all the experiments. Two peculiarities can be noted, namely the fact that the combination of parameters #2 resulted in a valley in terms of depth, meaning that the tool has cut less in depth, likely due to a slight misalignment, and secondly in every trial there is a progressive reduction of the depth from the start towards the end, with losses up to 80 µm, and this could be due to a high heat generated during continuous cutting and to tool deflection.

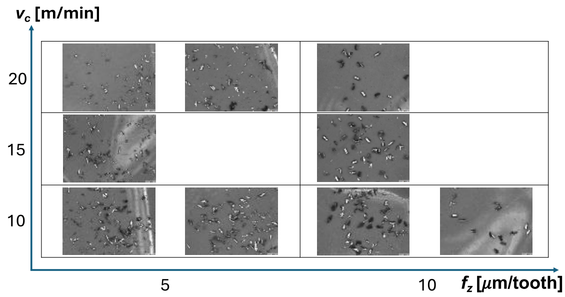

Fig. 13: Chips after micromilling and its parameters

The experiments consisting of micromachining straight lines on the previously AWJ milled channels with the best parameter combination (v_c=10 mm/min; f_z=5 µm/tooth) has shown the same results as in the reference surface in terms of burrs presence, chips formation, and geometrical accuracy.

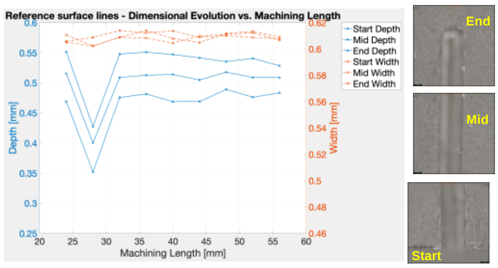

Fig. 14: Dimensional accuracy on reference surface

Moving to the assessment of the 4 mm spirals on the previously AWJ machined pockets, the results in terms of geometrical accuracy are presented in Fig. 15. The spirals widths and depths were measured in 8 different points shown on the right-hand side of Fig. 15, and they were machined with an equal new tool of 0.6 mm diameter, with the correspondent machining lengths shown in the legend. The geometrical accuracy of the spirals is not deteriorating with the increase of machining length, and it has shown consistent outcomes. The challenges of this type of experiments on the previously AWJ machined channels can be noticed from these measurements, that is the presence of the pockets' slopes due to the geometry of the AWJ milling process, resulting in regions were the tool cut more than expected in depth, and an evidence of which is represented by the peaks in the depth measurements graph outlined in Fig. 15. These zones where the tool was passing out of the flat bottom area, led to cuts inside the slope.

Furthermore, due to the nature of the AWJ process and its irregularity, the surface can present sloped regions from left to right in the direction parallel to the AWJ jet, and it is the case of 3 out of the spirals which led to loss of cut on the 7th point of measure as it can be seen from the valleys in the width measurements graph reported in Fig. 15.

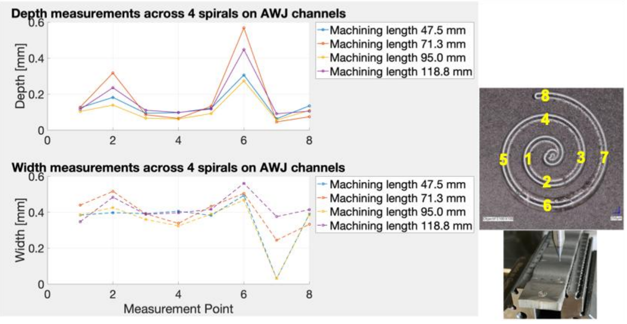

Fig. 15: Dimensional accuracy of micromilled spirals on AWJ channels

Besides, the chips collected from the experiments of spirals micromilling did not show evident difference across the different experiments, they are consistently continuous and of very similar dimensions, as it can be noticed from Fig. 16.

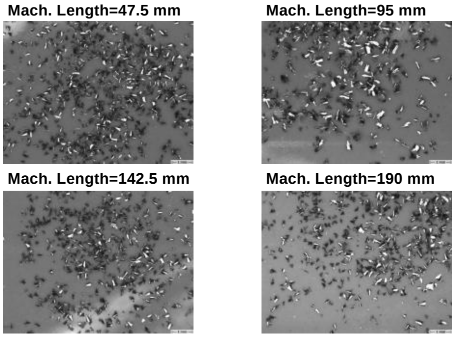

Fig. 16: Chips comparison - spirals on AWJ channels

7 CONCLUSIONS

The following list summarizes the different conclusions that can be made from the present study:

- The experiments have shown that the surfaces obtainable by means of the AWJ process on a Ti6Al4V alloy are strongly influenced, in their resulting quality in terms of accuracy and roughness, by the cutting pressure and the stand-off distance, and less on the pitch value, a confirmation of which has been found statistically through Response Surface Methodology.
- Higher cutting pressure in AWJ resulted in higher cutting depths of pockets and higher stand-off distance in lower depths of pockets (similar results were also found by [Sultan 2015]). Moreover, higher cutting pressure led to lower length ratio and higher roughness, whereas higher stand-off distance led to higher length ratio and higher roughness. Specific desired depth of AWJ machined pockets can be achieved with low roughness.
- Micromilling using dry cutting in previously AWJ machined pockets has shown positive results irrespective to the roughness level of the machined surface, resulting in cuts with low burr presence.
- For lower feed per tooth, the chips collected from the micromilling experiments were longer and more connected.
- The AWJ path has to be at least three times bigger than the maximum width and height of the micromilling spirals' path, in order to have longer and wider flat bottom regions and avoid loss of cut in micromilling due to slopes induced by the AWJ milling process.
- This research could be explored further by testing tools with smaller diameter than 0.6 mm for the sake of comparison between different tools. Moreover, future works could measure tool vibrations, to further control the process and because of different AWJ parameters.

8 REFERENCES

[Balazs 2021] Balazs, B.Z., Geier, N., Takacs, M. and Davim, J.P. A review on micro-milling: recent advances and future trends. The Int. J. of Adv. Manuf. Tech., 2021, Vol.112, pp 655–684. doi: 10.1007/s00170-020-06445-w

[Bui 2017] Bui, V.H., Gilles, P., Sultan, T. et al. A new cutting depth model with rapid calibration in abrasive water jet machining of titanium alloy. Int. J. of Adv. Manuf. Tech., 2017, Vol.91, pp 2465–2477. doi: 10.1007/s00170-017-0581-x

[Bui 2019] Bui, V.H., Gilles, P., Sultan, T. et al. Adaptive speed control for waterjet milling in pocket corners Int. J. of Adv. Manuf. Tech, 2019, Vol.101, pp 1381–1394. doi: 10.1007/s00170-019-03546-z

[Campos 2018] Campos, F. de O. Micromilling of Titanium Alloys: A Comparison Between Workpieces Produced by Casting, ECAP and 3D Printing (SLM). Doctoral thesis. Rio de Janeiro: Universidade Federal do Rio de Janeiro, COPPE, 2018

[Carou 2017] Carou, D., Rubio, E.M., Herrera, J., Lauro, C.H. and Davim, J.P. Latest advances in the micro-milling of titanium alloys: a review. Procedia Manufacturing, Vol.13, pp 275–282. doi: 10.1016/j.promfg.2017.09.071

[Dornfeld 2006] Dornfeld, D., Min, S. and Takeuchi, Y. Recent advances in mechanical micromachining. Annals of the CIRP, 2006, Vol.55, No.2, pp 745–768. doi: 10.1016/j.cirp.2006.10.006

[Jun 2019] Jun, Y., Lee, J., Choi, S., Yang, J.H., Sander, M., Chung, S. and Lee, S.H. In vivo–mimicking microfluidic perfusion culture of pancreatic islet spheroids. Science Advances, November 2019, Vol.5, eaax4520. doi: 10.1126/sciadv.aax4520

[Kim 2017] Kim, J.S., Kim, J.W. and Lee, S.W. Experimental characterization on micro-end milling of with chilly gas. International Journal of Advanced Manufacturing Technology, 2017, Vol.91, No.9–12, pp 2741–2749. doi: 10.1007/s00170-016-9965-6

[Kumar 2025] Kumar, D. and Srinivasu, D.S. Shallow-angled jet impingement generated channel geometry prediction in milling Ti-6Al-4V alloy. Journal of Manufacturing Processes, 2025, Vol.134, pp 410–434. doi: 10.1016/j.jmapro.2024.12.047

[Niknam 2014] Niknam, S.A., Khettabi, R. and Songmene, V. Machinability and machining of titanium alloys: a review. In: J.P. Davim, ed. Machining of Titanium Alloys, Heidelberg: Springer, pp 1–22.. doi:10.1007/978-3-662-43902-9_7

[Sultan 2015] Sultan, T.C. Usinage de metaux durs par Jet d'Eau Abrasif (in French). Toulouse: INSA de Toulouse, 2015. Available at: https://theses.hal.science/tel-01244408v1

[Thepsonthi 2014] Thepsonthi, T. and Özel, T. An integrated toolpath and process parameter optimization for high-performance micro-milling process of Ti–6Al–4V titanium alloy. Int. J. of Adv. Manuf. Tech., 2014, Vol.75, No.1–4, pp 57–75. doi: 10.1007/s00170-014-6102-2

[Veiga 2013] Veiga, C., Davim, J.P. and Loureiro, A.J.R. Review on machinability of titanium alloys: the process perspective. Reviews on Advanced Materials Science, 2013, Vol.34, pp 148–16